

Article

# CFD Model Studies of Dust Dispersion in Driven Dog Headings

Magdalena Tutak <sup>1</sup>, Jarosław Brodny <sup>2</sup>, Antoni John <sup>3</sup>, Janos Száva <sup>4,\*</sup>, Sorin Vlase <sup>4,5</sup>  
and Maria Luminita Scutaru <sup>4,\*</sup>

<sup>1</sup> Faculty of Mining, Safety Engineering and Industrial Automation, Silesian University of Technology, 41-800 Zabrze, Poland

<sup>2</sup> Faculty of Organization and Management, Silesian University of Technology, Roosevelta 26-28, 41-800 Zabrze, Poland

<sup>3</sup> Faculty of Mechanical Engineering, Silesian University of Technology, Konarskiego 18A, 44-100 Gliwice, Poland

<sup>4</sup> Department of Mechanical Engineering, Transilvania University of Brasov, B-dul Eroilor, 29, 500036 Brasov, Romania

<sup>5</sup> Romanian Academy of Technical Sciences, 010071 Bucharest, Romania

\* Correspondence: eet@unitbv.ro (J.S.); lscutaru@unitbv.ro (M.L.S.)

**Abstract:** Dust is one of the most burdensome hazards found in the environment. It is composed of crushed solids that pose a threat to the health and life of people, machines and machine components. At high concentration levels, it can reduce visibility. All of these negative phenomena occur during the process of underground mining, where dust hazards are common. The negative impact of dust on the efficacy of the mining process prompts research in this area. The following study presents a method developed for model studies of dust dispersion in driven dog headings. This issue is immensely important due to the fact that these dog headings belong to a group of unidirectional excavations (including tunnelling). This paper presents the results of model studies on dust dispersion in driven dog headings. The main focus is on the analysis of the distribution of dust concentration along a dog heading during the mining process. In order to achieve this goal, a model test method based on the finite volume method, which is included in the group of CFD methods, was developed. Analyses were carried out for two different values of dust emission from the face of the excavation for the transient state. The results made it possible to determine areas with the highest potential for dust concentration. The size and location of these areas are mainly dependent on the amount of dust emissions during the mining process. The results can support the process of managing dust prevention and protection of workers during the mining excavation process.

**Keywords:** dust dispersion; driven dog heading; CFD model; underground mining

**MSC:** 76B15



**Citation:** Tutak, M.; Brodny, J.; John, A.; Száva, J.; Vlase, S.; Scutaru, M.L. CFD Model Studies of Dust Dispersion in Driven Dog Headings. *Mathematics* **2022**, *10*, 3798. <https://doi.org/10.3390/math10203798>

Academic Editor: Elena Benvenuti

Received: 8 September 2022

Accepted: 12 October 2022

Published: 14 October 2022

**Publisher's Note:** MDPI stays neutral with regard to jurisdictional claims in published maps and institutional affiliations.



**Copyright:** © 2022 by the authors. Licensee MDPI, Basel, Switzerland. This article is an open access article distributed under the terms and conditions of the Creative Commons Attribution (CC BY) license (<https://creativecommons.org/licenses/by/4.0/>).

## 1. Introduction

One of the most commonly reported threats associated with the extraction of solid minerals in underground mines, including hard coal, is dust. In hard coal mines, this hazard results from the common occurrence of coal and hard dust in mining excavations (including a mixture of silica, aluminosilicates and other components, such as trace metals). The dust is produced in the process of mining and transporting the mine output [1–3]. The main reason for the formation of large amounts of dust in this process is current machining-based technology used for mining the rock mass. During this process, the rock is crushed and ground, which causes the formation of large amounts of rock and coal dust. In the case of mining operations, quantities of dust are directly proportional to the amount of the mine output.

In addition, large amounts of dust are generated during horizontal and vertical transport and repeated pouring of the mine output. The dust generated in the mining process is very dangerous for both employees and machines [4]. It floats in the mine atmosphere and can reach most mining excavation sites through a ventilation system, even those far from its place of origin. This causes the dust hazard to occur in virtually all mining excavations. However, the largest amount of dust can be found in excavations with unmined coal (coal body), including driven dog headings.

Dog headings (tunnels) driven in coal and rock belong to a group of the so-called “blind” or unidirectional excavations (Figure 1). This means that they only have one connection to the central (general) ventilation system. This, in turn, means that both fresh and exhaust air is transported through the same excavation. As a result, fresh air must be delivered to the face zone, where the rock mass is mined, in such a way that it does not impede the outflow of exhaust air and gases that are emitted into this dog heading from the rock mass.

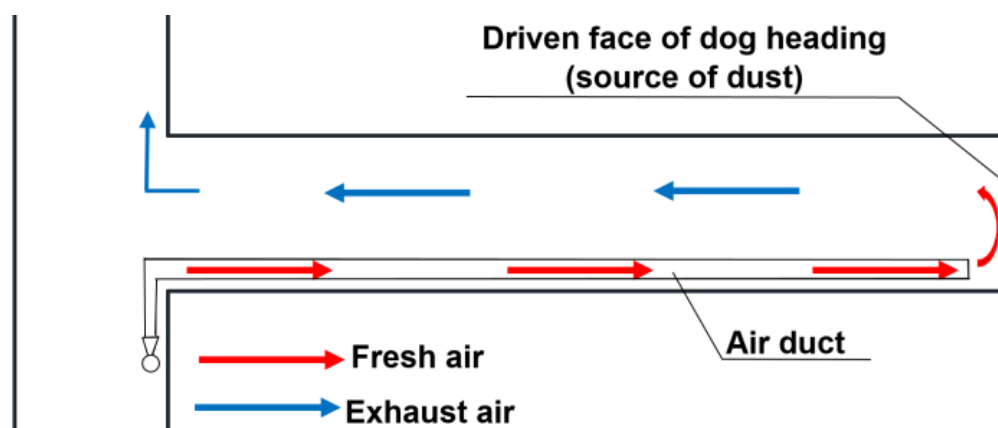


Figure 1. Ventilation diagram for a driven dog heading.

The face of such excavations is also characterized as having the greatest amount of dustiness [5]. In addition to profound harmfulness to employees' health, this dustiness also reduces visibility, leading to total darkness. This significantly hinders operations. Dust is also considered to have an immensely negative effect on the operation of machines and their individual elements. According to statistics, dust generated in the mining process accounts for 60–80% of the dust generated in the entire mine [5]. The presence of dust in mine workings poses a great threat to the health of workers, both physical and psychological, as well as to the environment. Additionally, high concentrations of dust are the cause of very dangerous dust explosions [5–8]. Thus, it can be assumed that dustiness, which cannot be eliminated in the mining production process, is a very unfavorable phenomenon both to the health and life of the crew and the efficiency of the mining process.

Due to the very unfavorable effects of dust in mine workings, this topic has been addressed by many researchers. For example, probability experiments, direct field measurements and numerical simulations have been used to study dust in mine workings. Experimental studies have been conducted on scaled simulation models, among other aspects. Tan et al. designed an experimental model for a fully mechanized face at the Tongxin coal mine. They conducted a study of the distribution of dust concentrations of different moisture contents generated during coal mining, casing shifting, collapse and coal transport [9]. In turn, Shi et al. developed an experimental model to analyze the variation of dust concentrations during coal mining at different ventilation air velocities [10]. The simplifications they introduced to the structure and environmental conditions resulted in large deviations from the actual measurement results.

In terms of direct measurements, it is worth mentioning a study [11] that measured the distribution of PM<sub>2.5</sub> dust concentrations in a coal face. Liu et al. carried out measurements

of changes in dust concentrations along a driven dog heading during coal mining in a fully mechanized coal face [12]. It should be noted that field studies also show a number of shortcomings, including issues related to measurement uncertainty and the influence of very harsh environmental conditions on the quality of these measurements. Oftentimes, however, the results of these measurements are used to validate the accuracy of analytical experiments and the numerical simulations carried out.

In the case of model studies (numerical simulations), measurements in real conditions are crucial for mapping the studied region and the air flow field and diffusion behavior of dust emitted from various sources. Therefore, it is clear that model studies using structural models are now becoming an alternative to studies under real conditions. They also provide extensive opportunities for multivariate analysis of different states of the phenomenon under study. Therefore, their application in underground mining is becoming increasingly widespread.

Due to these aspects, it is crucial to conduct research in the field in order to expand knowledge of dust dispersion in mining processes. In this regard, both on-site and real-life studies are conducted. Model studies are increasingly used to analyse phenomena that would be hard to examine in real conditions.

Nevertheless, the use of model studies to examine the phenomenon of dustiness requires analysing two media, namely a gas medium (Euler) and a solid medium (Lagrange). Therefore, the analysis of dust dispersion in mining excavations requires a combination of gas and solid media.

The main objective was to determine a method of dust dispersion in driven dog headings and its concentration levels along these dog headings during the mining process. In order to achieve this goal, a model study method based on the finite volume method was developed. The study was performed for the actual driven dog heading, and the ventilation parameters adopted as boundary conditions were obtained based on direct studies. The analyses covered two different values of dust emissions from the face of the driven dog heading and were carried out for the transient state. In addition to the emission of dust into driven dog headings, the study also looked at the release of methane from the excavated coal seam, which makes it possible to reflect the actual ventilation processes in underground mine workings.

An important problem when modeling dust issues, including those in mine workings, is the issue of particle size distribution. This problem is extremely complex and depends on the type of seam being excavated and its geological properties, as well as the condition of the knives of the excavating machine organ and the process of sprinkling the seam. The analysis presented here adopts the distribution of dust particles according to the Rosin–Ramler model, often used in studies of dusting processes. This distribution is used to describe the diameter distribution of dust particles (materials) from processes such as grinding, milling, mincing and crushing, as well as for the diameter distribution of particles formed in other processes [13–17].

Adopting this model for the distribution of dust particles, taking into account the release of methane and analyzing the pumping system represent a new approach to the problem under study.

The ANSYS Fluent software was utilized for the analysis, which enabled the authors to determine the parameters of the mine gas and dust mixture at individual points of the studied dog heading (in a spatial arrangement).

## 2. Materials and Methods

The analysis of the impact of dust mass expenditure (quantity) on the dustiness of the driven dog heading was conducted using the computational fluid mechanics (CFD) in the Ansys Fluent software. In order to model a biphasic system, i.e., gas and solid, the Eulerian–Lagrangian approach was used. This approach assumes that the gas phase is regarded as a continuum by solving the Navier–Stokes equation, while the dispersed (dust)

phase is solved by tracking the movement of a large number of particles in the calculated continuous phase field.

In accordance with the principles of fluid mechanics, the flow of air stream (gas) through the studied driven dog heading was adopted as a continuous phase, and dust was adopted as a discrete phase.

### 2.1. Mathematical Model of the Gas Flow through a Dog Heading

The mathematical model of airflow consists of conservation equations of turbulent mass, momentum, species and energy, as well as the scalar transport equations for the turbulence model [18,19]:

$$\nabla \cdot \rho U = 0 \tag{1}$$

$$\nabla \cdot \rho U U = \nabla \cdot \sigma + \rho g \tag{2}$$

where:

$$\sigma = -pI + [(\mu + \mu_t)(\nabla U + (\nabla U)^T)] - \frac{2}{3}(((\mu + \mu)(\nabla \cdot U)I) \rho k I) \tag{3}$$

$$\nabla \cdot (\rho c_p U T) = \nabla \cdot \left( k_{eff} + \frac{c_p \mu_t}{Pr_t} \right) \nabla T \tag{4}$$

$$\nabla \cdot (\rho \omega_i U) = \nabla \cdot \left( \rho D_{i,eff} + \frac{\mu_t}{Sc_i} \right) \nabla \omega_i \tag{5}$$

where:  $\rho$  is gas density (kg/m<sup>3</sup>);  $U$  is air velocity (m/s);  $p$  is pressure (Pa);  $g$  is gravity acceleration (m·s<sup>-2</sup>);  $\omega_i$  is mass fraction of species  $i$ ;  $\mu/\mu_t$  are dynamic viscosity, Pa·s<sup>-1</sup>;  $T$  is temperature, K;  $Sc_i$  is the Schmidt number;  $Pr_t$  is Prandtl number;  $k_{eff}$  is effective thermal conductivity, W·m<sup>-1</sup>·K<sup>-1</sup>; and  $D_{i,eff}$  is effective diffusivity of species  $i$ , m·s<sup>-2</sup>.

The stream of the air flowing through driven dog headings is turbulent in nature. In order to model the turbulent flow, the  $k$ - $\epsilon$  model was used. This model is based on solving Navier–Stokes equations averaged over time (the so-called RANS equation—Reynolds-Averaged Navier–Stokes). These equations are incomplete; hence, it is necessary to solve the variables  $k$ —the so-called kinetic turbulence energy and  $\epsilon$ —energy dissipation, which were introduced to close the equations. The equation of kinetic turbulent energy and the equation of kinetic turbulent energy dissipation can be expressed as follows [20]:

$$\frac{\partial}{\partial t} \frac{\partial k}{\partial t} + \frac{\partial}{\partial x_i} (\rho k u_i) = \frac{\partial}{\partial x_j} \left[ \left( \mu + \frac{\mu_t}{\sigma_k} \right) \frac{\partial k}{\partial x_j} \right] + G_k + G_b - \rho \epsilon - Y_M + S_k \tag{6}$$

$$\frac{\partial}{\partial t} \frac{\partial \epsilon}{\partial t} + \frac{\partial}{\partial x_i} (\rho \epsilon u_i) = \frac{\partial}{\partial x_j} \left[ \left( \mu + \frac{\mu_t}{\sigma_\epsilon} \right) \frac{\partial \epsilon}{\partial x_j} \right] + C_{1\epsilon} \frac{\epsilon}{k} (G_k + C_{3\epsilon} G_b) - C_{2\epsilon} \rho \frac{\epsilon^2}{k} + S_\epsilon \tag{7}$$

where:  $C_{1\epsilon}$ ,  $C_{2\epsilon}$ ,  $C_{3\epsilon}$  are constants;  $\sigma_k$ ,  $\sigma_\epsilon$  are turbulent Prandtl numbers for  $k$  and  $\epsilon$ ;  $G_b$  is the generation of turbulence kinetic energy due to buoyancy;  $G_k$  is the generation of turbulence kinetic energy due to the mean velocity gradients;  $Y_M$  is a contribution of the fluctuating dilatation in compressible turbulence to the overall dissipation rate; and  $S_k$ ,  $S_\epsilon$  are user-defined source terms.

### 2.2. Mathematical Model of the Coal Dust Flow through a Dog Heading

The Lagrange method is used to track the trajectory of DPM particles. In this method, the motion of particles takes place according to Newton’s second law. The movement of dust particles is influenced by many forces, which makes their interactions extremely complex. These forces mainly include gravity, adhesive force, drag force, buoyancy force, Magnus force, Saffman force, Basset force and False mass force [21]. However, since many of these interactions are small, most of them are ignored, with resistance force, gravity and pressure gradient force predominantly taken into account. According to Newton’s second

law, the force acting on a single dust particle can be determined based on the following relationship [22–26]:

$$m_p \frac{dv_p}{dt} = F_{drag} + F_g \quad (8)$$

where:  $m_p$  is the mass of dust particles (kg);  $v_p$  is the velocity of dust particles (m/s);  $F_{drag}$  is the drag force on the particles, (N); and  $F_g$  is gravity (N).

Therefore,  $F_{drag}$  is expressed as:

$$F_{drag} = \frac{\frac{1}{8} C_d \rho \pi d_p^2 |v - uv_p|}{v - v_p} \quad (9)$$

where:  $d_p$  is the particle diameter (m);  $u$  is the air velocity (m/s);  $v_p$  is the particle velocity (m/s); and  $C_d$  is the drag coefficient.

Therefore,  $C_d$  is given as:

$$C_d = \begin{cases} \frac{24}{Re \cdot C_c} & \text{for } Re \leq 1 \\ \frac{24(1+0.15Re^{0.687})}{Re} & \text{for } 1 < Re \leq 1000, \\ 0.44 & \text{for } Re > 1000 \end{cases} \quad (10)$$

where:  $C_c$  is the Cunningham slip correction factor, which is expressed by:

$$C_c = 1 + \frac{\lambda}{d_p} \left( 2.514 + 0.8e^{-\frac{0.55d_p}{\lambda}} \right), \quad (11)$$

where:  $\lambda$  is the mean free path of gas molecules.

Velocity of dust particles with different sizes can be calculated by the following equation:

$$v_p = \sqrt{\frac{4(\rho_p - \rho_g)gd_p}{3\rho_g C_d}}, \quad (12)$$

### 3. Problem Statement and Boundary Conditions

The basis for the numerical analysis was the dog heading model with its real geometry, ventilation parameters (measured in real conditions) and equipment. The geometrical parameters along with the location of the auxiliary air duct line are shown in Figure 2. The diameter of the air duct line was 0.6 m. The air outlet of the air duct line was located 5.0 m from the mined coal body. The air duct line was built at a height of 2.5 m, and 0.65 m from the side wall of the dog heading (Figure 2). The source of dust was located on the surface of the mined coal body (as in reality).

The study was conducted for a forced (air-duct) ventilation system through pressing. This system is characterized by more intensive removal of noxious gases from the face than in the case of suction or combined ventilation, lower air losses and more favorable climatic conditions in the excavation. The disadvantage of this system is that used air flows through the entire length of the excavation, which causes difficulties in removing methane gas emitted from the excavated face, which tends to accumulate under the roof. With suction ventilation, the dilution of gases is faster, and the conditions in the entire excavation are more favorable because the gases do not flow out through the excavation, but through the air-duct ventilation. Combined ventilation, on the other hand, combines the advantages of suction and press ventilation. It is implemented by changing the direction of rotation of the axial fans' impeller, using a reversible device or two fans and bolts.

As previously mentioned, a pumping (pressing) system was used in this study. After developing a geometric model and defining boundary conditions (Figure 2), discretization of the developed model was carried out. This consisted of generating a polyhedral mesh consisting of a finite number of control volumes (Figure 3).

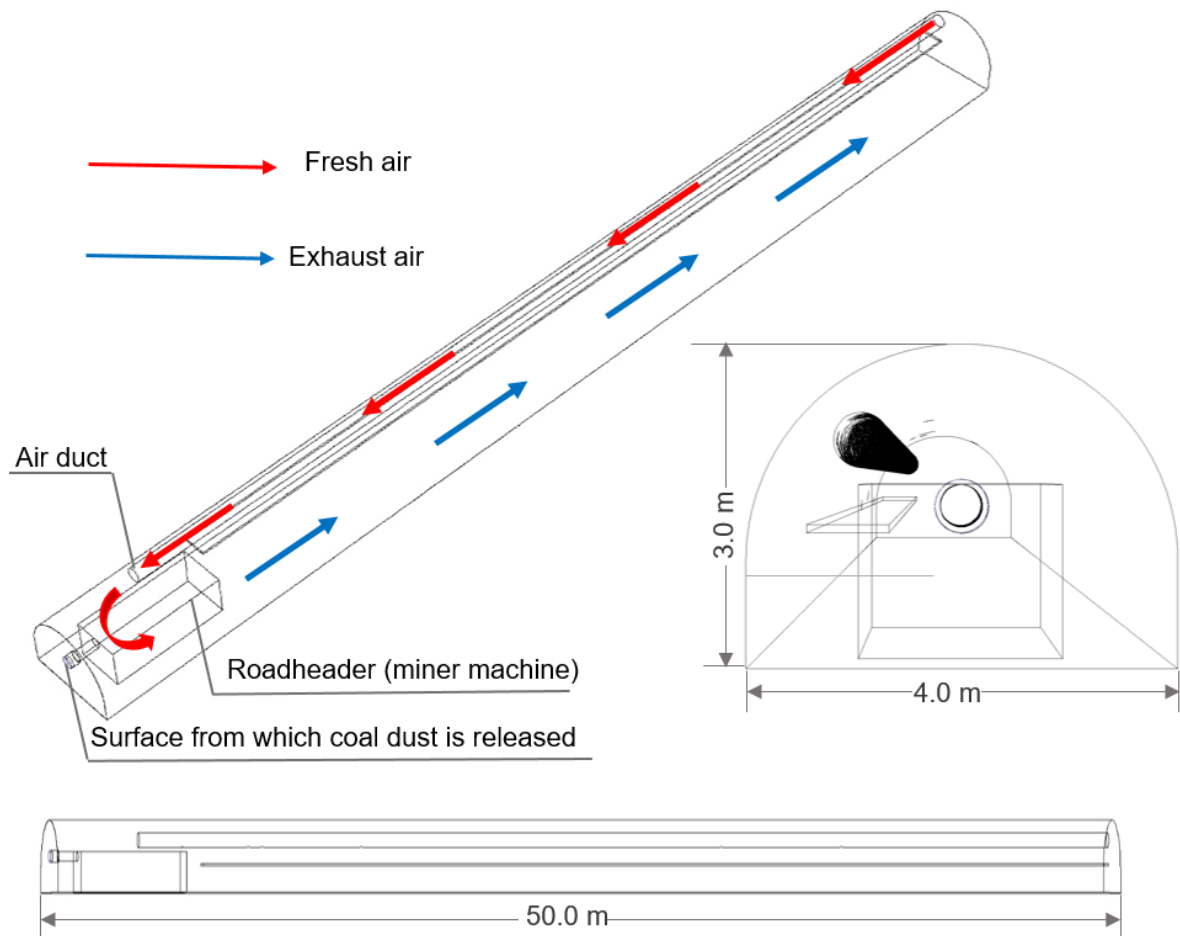


Figure 2. Geometric model of the studied dog heading with marked air flow directions.

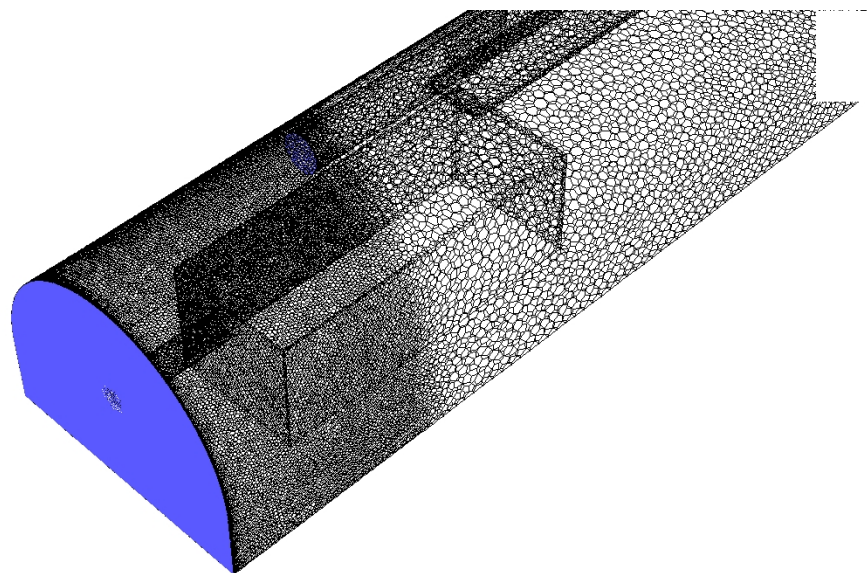


Figure 3. Fragment of the discrete model of the studied dog heading.

The boundary conditions were then adopted, including the physical model, which was used for numerical calculations. The basic parameters of the calculation model are shown in Table 1.

**Table 1.** The major parameter setting.

Name	Parametr Setting
Solver Type	Pressure-Based
Viscous Model	k-epsilon
Diameter Distribution	Rosin-Rammler
Total Flow Rate, kg/s	0.00125/0.00075
Material	Coal-hv
Max Diameter, m	0.001
Min Diameter, m	0.000001
Mean Diameter, m	0.0005
Density of dust, kg/m <sup>3</sup>	1200

Calculations were made for the transient state. The analysis time was 180 s. Two variants of the emission volume of dust produced during the driving of the dog heading were analysed: 0.00125 and 0.00075 kg/s.

For each of the studied variants, the air flow delivered to the driven dog heading by means of the air duct line was the same and amounted to 376.8 m<sup>3</sup>/min.

The research focused on the analysis of dust dispersion in the face zone from the commencement of mining the coal body. It was assumed that dust was released into the dog heading from the fragment of mined forehead. The dust grain composition was described according to the Rosin–Rammler distribution.

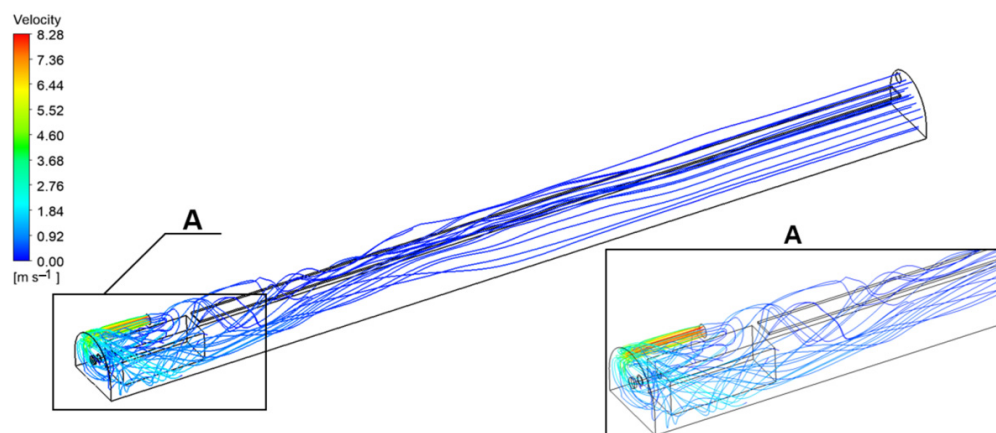
Numerical studies were conducted using Ansys Fluent 19.2 software (Canonsburg, PA, USA).

#### 4. Results and Discussions

Research on the impact of the mass expenditure (quantity) of dust released into the dog heading during mining was carried out for the model, in which the biphasic medium created from the continuous air phase and the discrete phase in the form of dust particles was taken into account. The analysis involved the interaction between these phases.

A number of interesting results were obtained regarding both the ventilation parameters of the air stream and the distribution of dust particles itself.

In the first stage, ventilation parameters were determined for the system without dust. The air flow trajectories (without dust) through the driven dog heading are shown in Figure 4.

**Figure 4.** Trajectories of air flowing through the driven dog heading (without dust).

Based on the results, the highest air velocity was reported to occur in the face zone of the driven dog heading, in the area of the air stream outlet from the air duct line. It was also found that there was an area of significant air recirculation in this zone, where the air flow was most turbulent. This is due to the fact that in this area, the air flowing out of the air duct line hits the mined coal body and is bounced off, thereby changing its return flow. At the same time, having bounced off the air duct line, the air stream encounters an obstacle in the form of a road header.

In the second stage, the study looked at the impact of mass expenditure (quantity) of dust released into the dog heading during mining on the level of dustiness.

Here, the focus was placed on the increase of dustiness in the face zone during mining. During the analysis, dust dispersion in the studied dog heading was determined, with its emission intensity being 0.00125 and 0.00075 kg/s, respectively. Dustiness in subsequent phases of the analysis with consideration of the size of dust particles is presented in Figures 5 and 6.

The results of the calculations help to trace changes in the level of dustiness in the studied dog heading with the passage of time for both studied emissions. It is also possible to trace how the dust spreads along with the moving air stream. The results also allow for the determination of the location of individual dust grains for the selected timeframe. It is clear that the greater the distance from the face of the dog heading, the smaller the dust particles that move with the air stream will be. In turn, the larger dust particles fall on the footwall of the dog heading, which is caused by the force of inertia. This phenomenon is dangerous to the health of the workers, because these pathogenic particles of the smallest diameter are transferred over considerable distances and are inhaled.

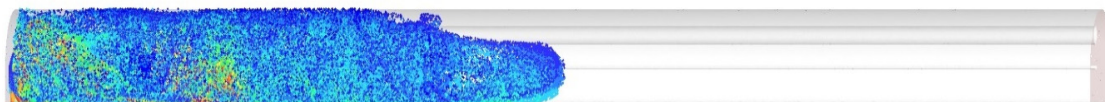
Dust concentration levels in vertical cross-sections of the dog heading for both emissions are presented in Figures 7 and 8. They are shown in cross-sections of the dog heading located every 5.0 m from the exposed surface of the mining area (for 10 cross-sections).

Based on the results, the authors were able to determine changes in dust concentration levels along the measurement line located in the central plane of the dog heading at a height of 1.75 m (average height of the human mouth and nose) from its base. Distributions were determined after the total analysis time (180 s) for both studied emissions at 10 points located on this line (Figure 9).

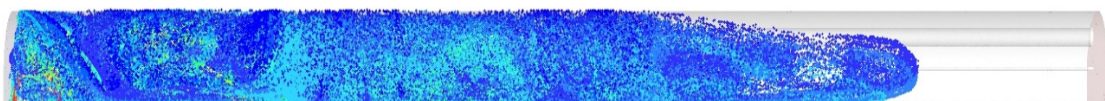
$t = 10$  s



$t = 60$  s



$t = 120$  s



$t = 180$  s

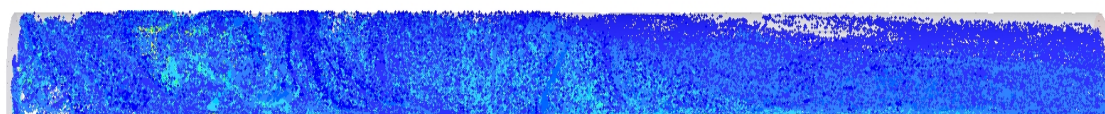


**Figure 5.** Distribution of different-sized dust particles in the dog heading at various time points for total dust rate = 0.00125 kg/s.

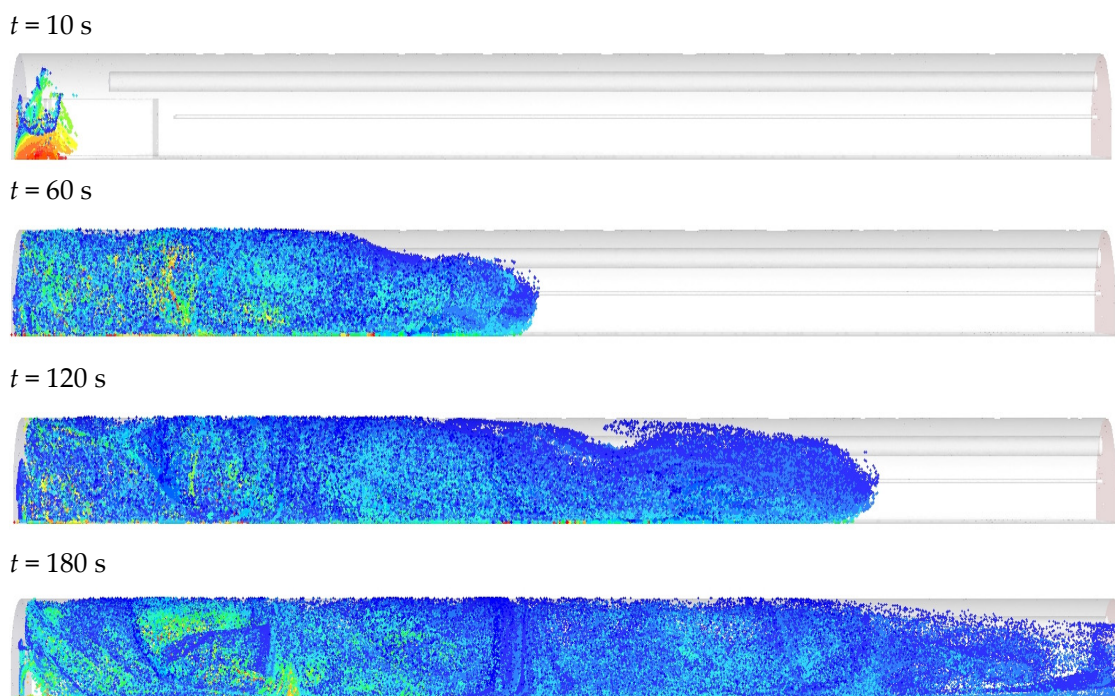


**Figure 6.** Distribution of different-sized dust particles in the dog heading at various times for total dust rate = 0.00075 kg/s.

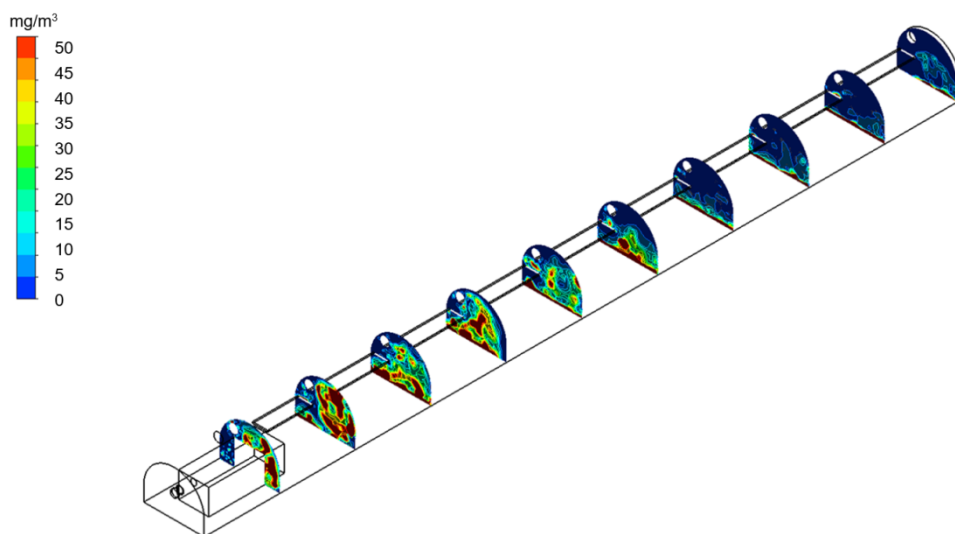


**Figure 7.** Mass dust concentration in the dog heading for time analysis  $t = 180$  s for total dust rate = 0.00125 kg/s.

The presented methodology of the research procedure and the results obtained complement the previous level of knowledge in the field of modeling the flow of air with dust through driven dog headings. Previous research in this area has focused on modeling the air flow and determining the trajectories of the overflow for various ventilation systems and the release of methane into them from the mined coal seam. These studies were carried out for steady-state flow. On the other hand, the analyses presented in this paper represent the first stage of research on dust dispersion in mine workings for conditions in underground coal mines. The undoubted advantage is the inclusion of transients in the analysis, which has not been used for this type of condition. Thus, there are no methods analyzing the presented condition. By contrast, similar analyses have been carried out for the combustion process and for turbulent flows with a dispersive phase [27–31].

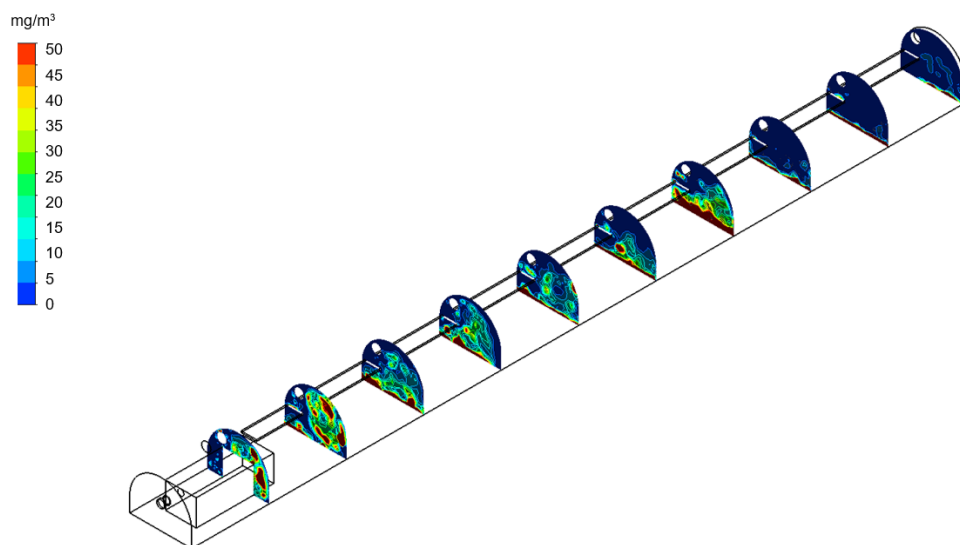


**Figure 8.** Mass dust concentration in the dog heading for time analysis  $t = 180$  s for total dust rate = 0.00075 kg/s.

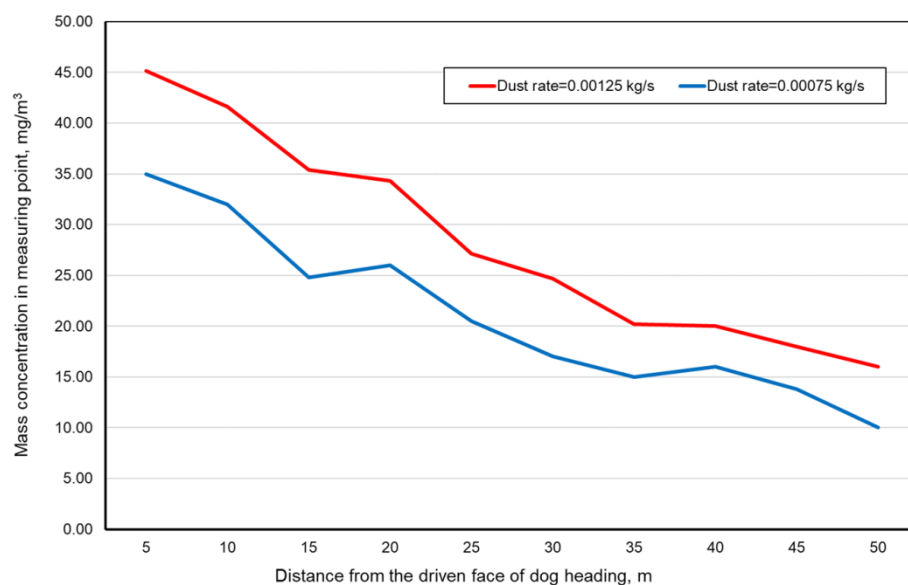


**Figure 9.** Distribution of dust concentration along the adopted measurement lines for studied variants.

### 5. Conclusions

Dust emissions from both mining and tunnel excavations constitute a major technical, organizational and health problem. Unfortunately, this dust has immensely harmful effects on the mining process. In order to reduce these effects, it is necessary to take measures to reduce dust emissions and movement in excavations. For this reason, it is important to know how dust disperses and distributes over time for various ventilation parameters. The method developed and presented in this paper allowed the authors to conduct such studies. However, it required an analysis of a biphasic medium with interaction. This approach makes it possible to trace the movement of dust particles in a gaseous medium for various ventilation parameters and the intensity of such emissions.

The method presented in this paper enables the determination of many interesting parameters of the gas–dust mixture. Undoubtedly, it creates opportunities for a much broader analysis of the phenomenon of dustiness in various areas and during various processes.

The results clearly indicate that the main reason for dust dispersion in mining excavations is an active ventilation system that transports dust particles over considerable distances from the place of their formation. The analysis of the distribution of this dust and trajectories of individual grains shows that its concentration is very uneven. This distribution largely depends on dust grain composition, the volume of emissions and ventilation parameters.

Based on the findings, it can be concluded that:

- (1) The highest concentrations of dust during the mining of the coal seam were reported at the face of the driven dog heading. Due to the ventilation system used for such a heading (press–air-duct ventilation), the diffusion of dust with high concentrations along the length of this excavation was significant.
- (2) The lowest dust concentrations, regardless of the size of dust emissions during the mining process, was reported on the side of the heading without a built-in air-duct ventilation system. This is because this side is where the air flows through the entire heading.
- (3) A significant decrease in dust concentrations was reported at a distance of about 40 m from the seam being mined in the heading.

These conclusions should be widely used by the services responsible for mine safety.

The presented methodology, based on numerical simulations, makes it possible to conduct a multivariate analysis of the state of dustiness, taking into account various parameters of the studied phenomenon. The universality of this methodology also allows its application for the analysis of dustiness, including dust reduction agents.

**Author Contributions:** Conceptualization, M.T., J.B. and A.J.; methodology, M.T. and J.B.; software, M.T. and J.B.; validation, M.T. and J.B.; formal analysis, M.T. and J.B.; investigation, M.T., J.B., A.J. and J.S.; resources, M.T. and J.B.; data curation, M.T., J.B. and A.J.; writing—original draft preparation, M.T., J.B., A.J. and M.L.S.; writing—review and editing, M.T. and J.B.; visualization, M.T. and J.B.; supervision, M.T. and J.B.; project administration, M.T., J.B. and J.S.; funding acquisition, J.S., M.L.S. and S.V. All authors have read and agreed to the published version of the manuscript.

**Funding:** This research received no external funding. The APC was funded by Transilvania University of Brasov.

**Data Availability Statement:** Not applicable.

**Conflicts of Interest:** The authors declare no conflict of interest.

## References

1. Brodny, J.; Tutak, M. Exposure to Harmful Dusts on Fully Powered Longwall Coal Mines in Poland. *Int. J. Environ. Res. Public Health* **2018**, *15*, 1846. [[CrossRef](#)] [[PubMed](#)]
2. Lebecki, K.; Małachowski, M.; Sołtysiak, T. Continuous dust monitoring in headings in underground coal mines. *J. Sustain. Min.* **2016**, *15*, 125–132. [[CrossRef](#)]
3. Ren, T.; Wang, Z.; Zhang, J. Improved dust management at a longwall top coal caving (LTCC) face—A CFD modelling approach. *Adv. Powder Technol.* **2018**, *29*, 2368–2379. [[CrossRef](#)]
4. Lilic, N.; Cvjetic, A.; Knezevic, D.; Milisavljevic, V.; Pantelic, U. Dust and Noise Environmental Impact Assessment and Control in Serbian Mining Practice. *Minerals* **2018**, *8*, 34. [[CrossRef](#)]
5. Wang, Z.; Li, S.; Ren, T.; Wu, J.; Lin, H.; Shaung, H. Respirable dust pollution characteristics within an underground heading face driven with continuous miner—A CFD modelling approach. *J. Clean. Prod.* **2019**, *217*, 267–283. [[CrossRef](#)]
6. Zhang, G.; Sun, B.; Song, S.; Wang, H.; Zhou, G. CFD comparative analysis on the pollution characteristics of coal dust under turbulent airflow from coal cutting in the fully mechanized mining face. *Process Saf. Environ. Prot.* **2021**, *146*, 515–530. [[CrossRef](#)]
7. Cai, P.; Nie, W.; Hua, Y.; Wei, W.; Jin, H. Diffusion and pollution of multi-source dusts in a fully mechanized coal face. *Process Saf. Environ. Prot.* **2018**, *118*, 93–105. [[CrossRef](#)]
8. Zhou, G.; Zhang, Q.; Bai, R.; Fan, T.; Wang, G. The diffusion behavior law of respirable dust at fully mechanized caving face in coal mine: CFD numerical simulation and engineering application. *Process Saf. Environ. Prot.* **2017**, *106*, 117–128. [[CrossRef](#)]
9. Tan, C.; Jiang, Z.-A.; Chen, J.-S.; Wang, P. Numerical simulation of influencing factors on dust movement during coal cutting at fully mechanized working faces. *Beijing Keji Daxue Xuebao/J. Univ. Sci. Technol. Beijing* **2014**, *36*, 716–721.
10. Shi, X.-X.; Jiang, Z.-A.; Zhou, S.-Y.; Cai, W. Experimental study on dust distribution regularity of fully mechanized mining face. *Meitan Xuebao/J. China Coal Soc.* **2008**, *33*, 1117–1121.

11. Nie, B.-S.; Li, X.-C.; Yang, T.; Hu, W.-X.; Guo, J.-H. Distribution of PM2.5 dust during mining operation in coal workface. *Meitan Xuebao/J. China Coal Soc.* **2013**, *38*, 33–37.
12. Liu, Y.; Jiang, Z.A.; Cai, W. Site measurement and digital simulation of dust density distribution in fully mechanized longwall coal mining face. *J. Coal Sci. Technol.* **2006**, *34*, 80–82.
13. Colorado-Arango, L.; Menéndez-Aguado, J.M.; Osorio-Correa, A. Particle Size Distribution Models for Metallurgical Coke Grinding Products. *Metals* **2021**, *11*, 1288. [[CrossRef](#)]
14. Hossein, A.; Gholamreza, S. Investigating the shape and size distribution of dust in mechanized longwall method in Tabas coal mine. *Hum. Ecol. Risk Assess. Int. J.* **2017**, *23*, 28–39.
15. Coello-Velázquez, A.L.; Quijano Arteaga, V.; Menéndez-Aguado, J.M.; Pole, F.M.; Llorente, L. Use of the Swebrec Function to Model Particle Size Distribution in an Industrial-Scale Ni-Co Ore Grinding Circuit. *Metals* **2019**, *9*, 882. [[CrossRef](#)]
16. Papáček, Š.; Petera, K.; Císař, P.; Stejskal, V.; Saberioon, M. Experimental & Computational Fluid Dynamics Study of the Suitability of Different Solid Feed Pellets for Aquaculture Systems. *Appl. Sci.* **2020**, *10*, 6954.
17. Li, B.; Zeng, M.; Wang, Q. Numerical Simulation of Erosion Wear for Continuous Elbows in Different Directions. *Energies* **2022**, *15*, 1901. [[CrossRef](#)]
18. Kurnia, J.C.; Sasmito, A.P.; Mujumdar, A.S. CFD simulation of methane disperse, on and innovative methane management in underground mining faces. *Appl. Math. Model.* **2014**, *38*, 3467–3484. [[CrossRef](#)]
19. Sasmito, A.P.; Birgersson, E.; Ly, H.C.; Mujumdar, A.S. Some approaches to improve ventilation system in underground coalmines environment—A computational fluid dynamic study. *Tunn. Undergr. Space Technol.* **2013**, *34*, 82–95. [[CrossRef](#)]
20. Ansys Fluent 12.0 Theory Guide. Available online: [https://www.afs.enea.it/project/neptunius/docs/fluent/html/th/main\\_pre.htm](https://www.afs.enea.it/project/neptunius/docs/fluent/html/th/main_pre.htm) (accessed on 11 October 2022).
21. Hu, S.; Liao, Q.; Feng, G.; Huang, Y.; Shao, H.; Gao, Y.; Hu, F. Influences of ventilation velocity on dust dispersion in coal roadways. *Powder Technol.* **2020**, *360*, 683–694. [[CrossRef](#)]
22. Geng, F.; Gui, C.G.; Wang, Y.; Zhou, F.B.; Hu, S.Y.; Luo, G. Dust distribution and control in a coal roadway driven by an air curtain system: A numerical study. *Process Saf. Environ. Prot.* **2019**, *121*, 32–42. [[CrossRef](#)]
23. Geng, F.; Gang, L.; Wang, Y.C.; Li, Y.M.; Yuan, Z.L. Numerical investigation on particle mixing in a ball mill. *Powder Technol.* **2016**, *292*, 64–73. [[CrossRef](#)]
24. Lu, H.; Lu, L. CFD investigation on particle deposition in aligned and staggered ribbed duct air flows. *Appl. Therm. Eng.* **2016**, *93*, 697–706. [[CrossRef](#)]
25. Yao, G.X. Coarse Particle Settling Properties Study Based on Particle Analysis. Master's Thesis, Jiangxi University of Science and Technology, Ganzhou, China, 2012.
26. Cardu, M.; Clerici, C.; Morandini, A.; Ocella, E. An experimental research on the comminution law and work index in jaw. In Proceedings of the XVIII International Mineral Processing Congress, Sydney, NSW, Australia, 23–28 May 1993.
27. Lu, Y.; Akthar, S.; Sasmito, A.; Kurnia, J. Prediction of air flow, methane, and coal dust dispersion in a room and pillar mining face. *Int. J. Min. Sci. Technol.* **2017**, *27*, 657–662.
28. Eaton, J.K.; Fessler, J.R. Preferential concentration of particles by turbulence. *Int. J. Multiph. Flows* **1994**, *20*, 169–209. [[CrossRef](#)]
29. Eaton, J.K. Two-way coupled turbulence simulations of gas-particle flows using point-particle tracking. *Int. J. Multiph. Flow* **2009**, *35*, 792–800. [[CrossRef](#)]
30. Varaksin, A.Y. Fluid dynamics and thermal physics of two-phase flows: Problems and achievements. *High Temp.* **2013**, *51*, 377–407. [[CrossRef](#)]
31. Greifzu, F.; Kratzsch, C.; Forger, T.; Lindner, F.; Schwarze, R. Assessment of particle-tracking models for dispersed particle-laden flows implemented in OpenFOAM and ANSYS FLUENT. *Eng. Appl. Comput. Fluid Mech.* **2016**, *10*, 30–43.